Proceedings World Geothermal Congress 2005
Antalya, Turkey, 24-29 April 2005

Wave Propagation in Geothermal Reservoirs: a Finite-Difference Method

Tsuneo Kikuchi and Shinsuke Nakao

AIST Tsukuba Central 7, 1-1-1, Higashi

t-kikuchi@aist.go.jp, sh-nakao@aist.go.jp

Keywords: two phase zone, geothermal reservoir, elastic wave, modeling, finite-difference

ABSTRACT

In some geothermal systems, a two-phase vapor-dominated region is formed with producing geothermal fluids. Monitoring the distribution of the two-phase zones is essential to reservoir managements.

A microearthquake survey is one of the effective methods to monitor a geothermal reservoir. However, characteristics of the wave propagation in the two-phase zone are not sufficiently clarified.

We, thus, carry out the modeling of elastic waves with an explicit finite difference scheme and make an attempt to obtain the characteristics of the wave propagation in the two-phase vapor dominated region.

Recently, performances of PCs have been improved dramatically and a PC cluster, which is one kind of the distributed memory parallel computer, is developed easily by linking with some PCs via LAN. Therefore, we developed the PC cluster for the modeling of elastic waves described above.

In this paper, we describe the developed PC cluster briefly and results of the modeling on the 3-D model including only the liquid-dominated region in a reservoir prior to carry out the modeling of the vapor-liquid two-phase.

1. INTRODUCTION

There is a possibility that a two-phase vapor- or liquid-dominated region in a geothermal reservoir is formed associated with the decrease of the reservoir pressure because of the overproduction or the insufficient recharge of geothermal fluids. If a monitoring of the two-phase zone is carried out, we can obtain important data for an optimum production plan of geothermal fluids.

A gravity survey or a resisitivity survey is shown to be very useful for the monitoring of the geothermal reservoir Hashimoto et al., 2002, Horikoshi et al., 2001, Kikuchi et al., 2003, Yokoi et al., 2001. A microearthquake survey is also thought to be useful, but is not clearly shown. One reason is thought that characteristics of the wave propagation in a two-phase zone are not sufficiently clarified.

Therefore, we carry out a numerical modeling to clarify characteristics of the wave propagation using an explicit finite difference scheme on a synthetic 3-D model. After that, we plan to apply the results to real geothermal fields for monitoring two-phase zones.

For example, at Ogiri geothermal field in southern Kyushu, Japan, the growth of the two-phase zone in some parts of the field was reported (Goko, 2004). In this field, several microearthquake surveys have been conducted. Therefore, if we carry out the modeling on the Ogiri 3-D model, comparing the results of modeling with the results of microearthquake surveys may show manner of the development of two phase zones.

First we have developed a PC cluster using 5 PCs. Next, we added more 4 PCs to it. These PCs are almost same. Using this cluster, we carried out the modeling on small-sized synthetic 3-D models. The purpose of this modeling is to test the finite difference numerical code. Main contents of this paper are the results of these tests.

2. CONSTRUCTION OF PC CLUSTER

The PC cluster developed consists of one server PC and 8 compute hosts. The system software of this PC cluster is SCore5.6.1. Real World Computing Partnership has developed Score and PC Cluster Consortium administrates it presently.

Server PC provides the software development environment and some daemons managing the cluster run on the server. Parallel applications run on compute hosts. Server and compute hosts are linked via Gigabit Ethernet switching hub and form one network. Users of this PC cluster can

Table 1. Specification of server and compute hosts

	server	compute hosts	
		initial-4 PCs	additional-4 PCs
CPU	Pentium 2	Pentium 4 2GHz	Pentium 4 2GHz
amount of memory (MB)	256	512 SDRAM-256MB (S133)x2	512 DDR SDRAM PC2100 -512MBx1
capacity of HDD(GB)	60	60	60
network interface	Gigabit Ethernet (Intel Pro/1000)	Gigabit Ethernet (Intel Pro/1000)	Gigabit Ethernet (Intel Pro/1000)

reach this network from the outside through a router. The specifications of server and compute hosts are shown in Table 1.

We show the reduction computation time if we use the PC cluster compared to the single PC in Figure 1. CPU of the single PC is Intel Pentium III□730MHz□and the amount of memory installed is 512MB.

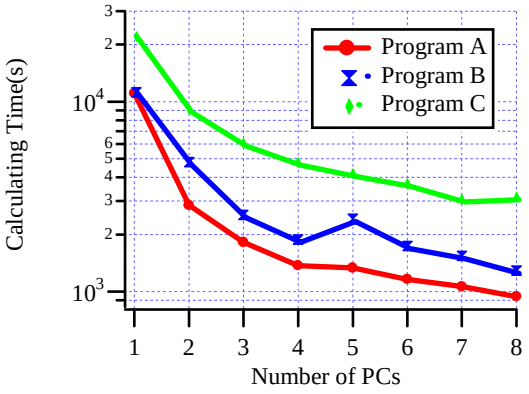

Figure 1. Relationship between the number of PCs and the total computation time.

We used three 3-D explicit finite difference programs for measurements of computation time. Scheme of these three programs is the staggered finite-difference method. Program A is second order accuracy in space and time, without intrinsic attenuation. Program B has fourth order accuracy in space, second order accuracy in time, without intrinsic attenuation. Program C has fourth order accuracy in space, second order accuracy in time, with intrinsic attenuation. All programs are C language programs.

As a whole, total computation time for every program reduces with increasing the number of PCs with one exception. Computation time for program B increases when the number of PCs increases 4 to 5.

As the configuration of this PC cluster, additional 4 PCs work if users attempt to use four and below PCs. If the number of PCs to be used is more than 5, initial PCs begin to work. All PCs have same CPU, but specifications of main board and memory are different between initial and additional PCs. Performances of additional PCs are a little higher than initial PCs. This may be the reason for the behavior described above. Other factor may affect the differences among three programs.

3. FINITE-DIFFERENCE PROGRAM AND MODEL

In this modeling, We use parallelized program A. Parameters used in calculations are as follows: grid spacing is the same in all directions, grid spacing Δx in x direction is 5 m, and time step Δt is 0.8 ms.

A model shown in Figure 2 is a cube 1 km on a side. We adopted absorbing boundaries around the model without top surface. Coordinate system is Cartesian coordinate and the coordinate origin is the upper left corner of the model. Downward direction in z-axis is positive.
A reservoir is located within this model. Dimensions of the reservoir are 250 m in width and depth, 125 m thick and the depth of top is 250 m deep from the top of the model. The

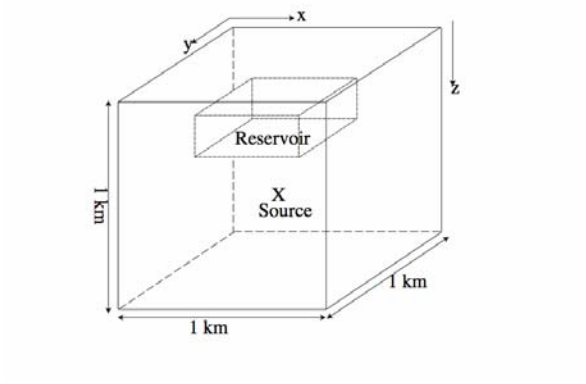

Figure 2. 3-D model including reservoir.

coordinate of the center of the reservoir is (x, y, z) = (500 m, 500 m, 312.5 m).

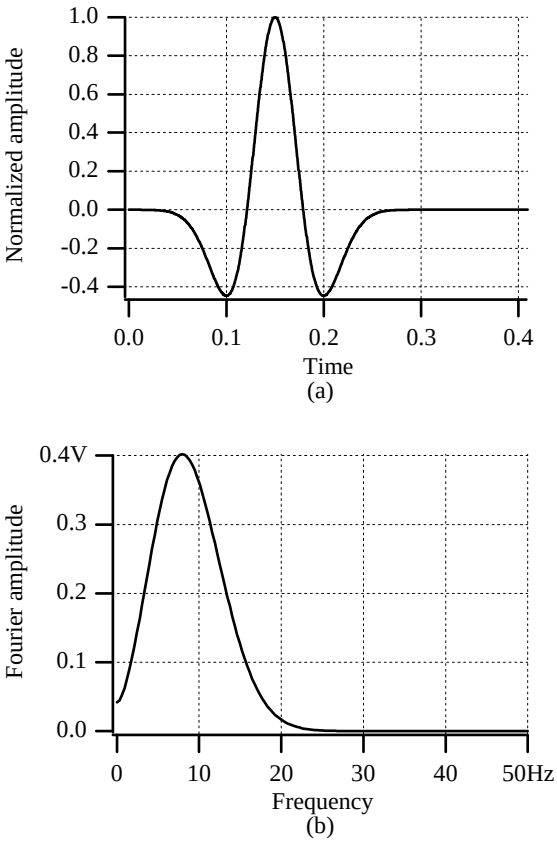

Figure 3. Source waveform and amplitude spectra. (a) waveform. (b) amplitude spectra.

At first, we verified the simulation program to work properly on a simple model. In particular, the reservoir includes 51 x 51 x 26 = 67626 gridpoints with the interval of 5 m and we specified some gridpoints, which are selected randomly, as water □acoustic velocity v_f=1500m/s, density ρ_f=1000kg/m^3□. However, these water gridpoints are not connected with each other in principle. In the homogeneous region except to the reservoir, we set P wave velocity v_p=3000m/s, S wave velocity v_s=1732m/s, density ρ=2300kg/m^3. This model does not intend to simulate the realistic situation and is simply a test of the finite difference code.

The vertical displacement of Riccer wavelet was applied upward at (x, y, z) = (525 m, 500 m, 660 m) and downward at (x, y, z) = (525m, 500m, 665m). Figure 3(a) shows the waveform and 3(b) shows the amplitude spectra.

The receivers with the interval of 25 m were arranged along the line located in the center of the model surface (y= 500 m) parallel to the x-axis.

4. RESULTS

Figure 4(a) shows displacement waveforms for z-component without water gridpoints, 4(b) shows results of the model including 10 % water gridpoints observed at receivers. The horizontal axis is distance from the y-axis; the vertical axis is time in sec. There are differences between waveforms after 0.5 s.

Figure 5 shows displacement waveforms for z-component

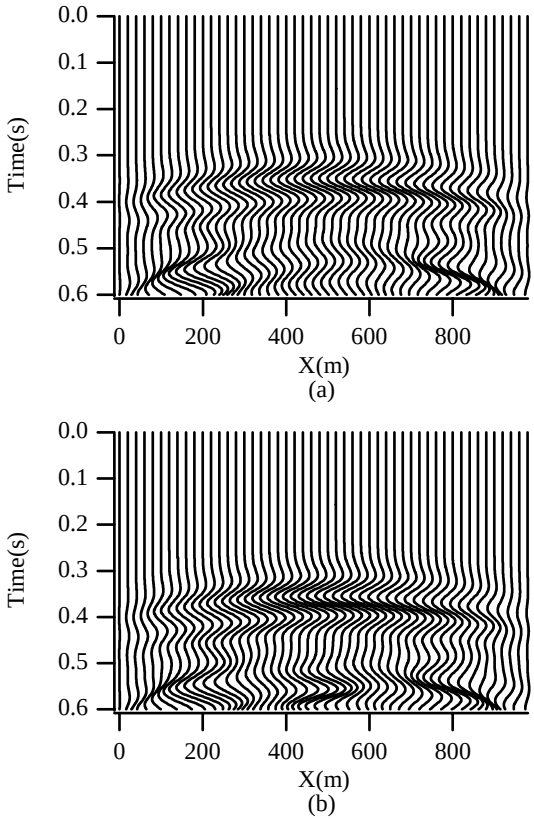

Figure 4. Displacement waveforms for z-component. (a) the model without water gridpoints. (b) the model including 10 % water gridpoints.

at (x, y) = (480 m, 500 m) from 0.2 s to 0.45 s. First arrival of direct P wave and direct S wave are involved in this period. First motion of direct P wave is 0.22 s□first motion of direct S wave is 0.37 s.

Solid line in Figure 5 shows the result of the model without water gridpoints, various dotted lines show the results of models with water gridpoints of 2%□4%□6%□8%□10%. The more percentage of water gridpoints increases, the larger amplitude and the more delay phase are observed.

Next, we carry out the modeling on the model which water gridpoints are connected with each other. Connected water gridpoints simulates a fracture. The length of a series of connected water gridpoints is up to 8. The number of

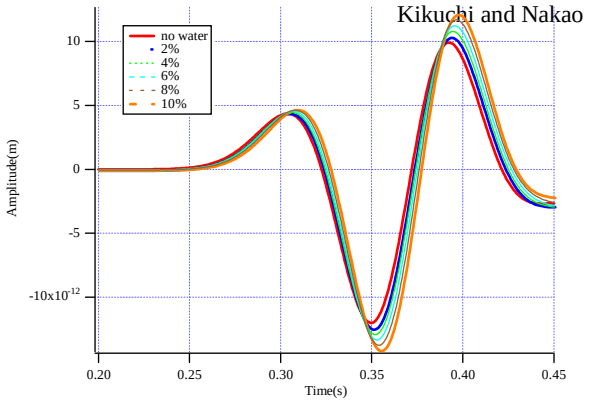

Figure 5. Displacement waveforms for z-component at (x, y) = (480 m, 500 m) from 0.2 s to 0.45 s. Red solid line shows no water gridpoints model. Various dotted lines show the results of models with water gridpoints of 2%□4%□6%□8%□10%.

connecting water gridpoints, azimuth and dip of a series of water gridpoints are decided by random numbers. However, a short series of water gridpoints is set to appear frequently.

In this model, the fracture is virtual and not realistic one. The maximum length of the fracture is about 40 m and the thickness of it is about 5 m because the grid spacing is 5 m. However, as a single fracture, the value of thickness is too large. It is simply assumed as a fracture zone or a fracture system. There are many literatures to describe modeling fractures in simulations (for example, Coates and Schoenberg, 1995, Pyrak-Nolte et al., 1990). We think the subject itself is very important and should be discussed further.

In this model, the total number of water gridpoints is 2279, corresponding to 3.4 % of the total reservoir gridpoints. Distribution of water gridpoints along x-z plain (y=500 m) is shown in Figure 6. Red dots are water gridpoints in the reservoir.

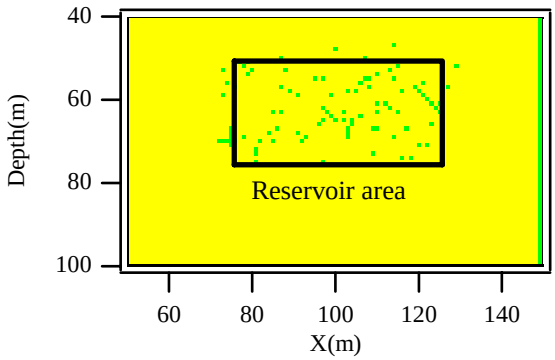

Figure 6. Distribution of water gridpoints (red dot) along x - z plain (y=500 m).

Figure 7 shows displacement waveforms for z-component observed at receivers. Snapshot of the displacement of z-component at 0.432 s along x-z plane (y=500 m) is shown in Figure 8. This snapshot shows the differences between the model including water gridpoints and the model of no water gridpoints. There is a large difference near the reservoir, suggesting a possibility to detect changes in reservoir properties.

5. CONCLUSIONS

We developed the PC cluster that consists of nine PCs for 3-D modeling of the elastic waves with a staggered explicit

finite difference scheme. If 8 PCs are used, the total computation time for three programs is one-half of 2 PCs case.

We carried out the modeling for the model that water grid points distribute randomly in the reservoir using this PC cluster. In this modeling, there is no unstable condition in computation process. Also, we obtained the appropriate results for the model which water gridpoints are connecting each other.

For future study, further modeling is planned in order to examine models with various percentage and distribution of water gridpoints, sources position, and etc.

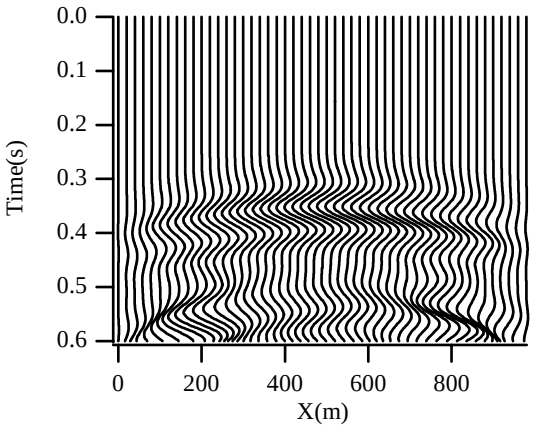

Figure 7. Displacement waveforms for z-component. Reservoir includes 3.4 % connected water grids.

REFERENCES

Coates, R. T. and Schoenberg, M. (1995): Finite-difference modeling of faults and fractures, Geophysics, Vol. 60, No. 5, pp. 1514 - 1526.

Goko, K. (2004): Towards sustainable steam production: the example of the Ogiri geothermal field, Vol. 26, No. 2, pp. 151 - 164 (in Japanese).

Hashimoto, K., Horikoshi, T. and Kikuchi, T. (2002): Development of Techniques for Reservoir Monitoring, 24th New Zealand geothermal workshop, pp. 109 - 114.

Horikoshi T., Yamasawa S., Ide T. and Tosha T. (2001): NEDO's Project on Development of Technology for Reservoir Mass and Heat Flow Characterization - Project Outline and Techniques to Improve the Reservoir Model. Geothermal Resources Council Transactions, Vol. 25, pp. 641 - 644.

Kikuchi, T., Horikoshi, T., Hashimoto, K., Nakagome, O., Shiga, N. and Yokoi, K. (2003): NEDO's Project on Development of Technology for Reservoir Mass and Heat Flow Characterization – Geophysical monitoring techniques -, Proceedings of The 6th SEGJ International Symposium, pp. 126 - 133.

Pyrak-Nolte, L. J., Myer L. R. and Cook, N. G. W., (1990): Transmission of seismic waves across single natural fractures, J. Geophys. Res., Vol. 95, No. B6, pp. 8617 - 8638.

Yokoi, K., Deguchi, T., Ide, T. and Tosha, T. (2001): Self-Potential Monitoring and Its Interpretation Using Numerical Reservoir Simulation at The Ogiri Geothermal Field, Japan, Geothermal Resources Council Transactions, Vol. 25, pp. 711 - 71.

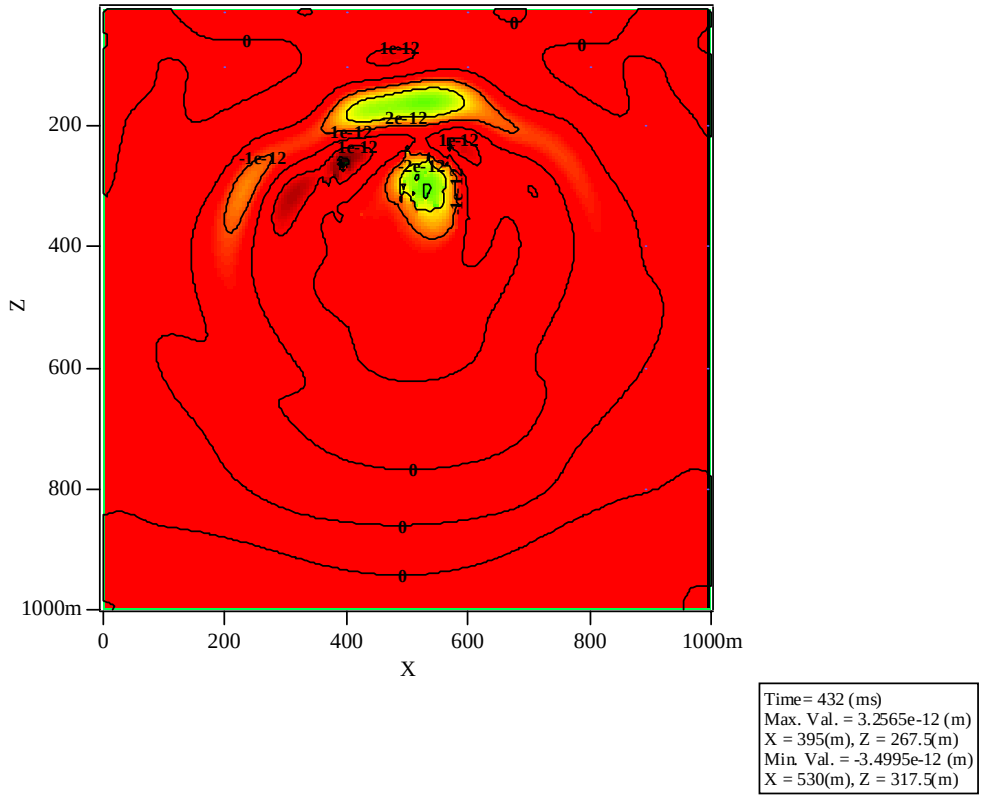

Figure 8. Differences of displacement for z-component at 0.432 s between the model including water gridpoints and the model of no water gridpoints.